

Automated Quantification and Topographical Distribution of the Whole Population of S- and L-Cones in Adult Albino and Pigmented Rats

Arturo Ortín-Martínez,^{1,2,3} Manuel Jiménez-López,^{2,3} Francisco M. Nadal-Nicolás,^{1,2} Manuel Salinas-Navarro,² Luis Alarcón-Martínez,² Yves Sauvé,^{4,5} Maria Paz Villegas-Pérez,² Manuel Vidal-Sanz,² and Marta Agudo-Barriuso^{1,6}

PURPOSE. To quantify the whole population of S- and L-cones in the albino (Sprague-Dawley, SD) and pigmented (Piebald Virol Glaxo, PVG) rats and to study their topographical distribution within the retina.

METHODS. Retinal radial sections and whole-mounted retinas were double immunodetected with antibodies against UV-sensitive and L-opsins to detect the S- and L-cones, respectively. Two automated routines were developed to quantify the whole population of S- and L-cones. Detailed isodensity maps of each cone type were generated. In both strains, the presence of dual cones was detected, these were semiautomatically quantified and their distribution determined. The matching distribution of retinal ganglion cells (RGCs) and L-cones was attained by double immunodetection of Brn3a and L-opsin, respectively

RESULTS. The mean number \pm SEM of L- or S-cones in SD and PVG retinas was $231,736 \pm 14,517$ and $239,939 \pm 6,494$ or $41,028 \pm 5,074$, and $27,316 \pm 2,235$, respectively. There was an increasing gradient of S-cone density along the inferonasal quadrant, although the highest densities were found in the retinal rims. The distribution of L-cones seemed to be complementary to the S-cones. The highest densities were observed in the superior nasotemporal axis, paralleling the distribution of Brn3a-positive RGCs.

CONCLUSIONS. These data establish, for the first time, the total number and the topographical distribution of S- and L-cones in two rat strains and demonstrate the correlation of L-cones and

RGC spatial distribution. (*Invest Ophthalmol Vis Sci.* 2010;51:3171-3183) DOI:10.1167/iovs.09-4861

In the mammalian retina, cone photoreceptors are responsible for daylight (photopic) vision and color discrimination. Color discrimination in nonprimate mammals is achieved by two types of cones: S and M/L. These cones are distinguished mainly by the portion of light spectrum to which each is more sensitive: short wave lengths stimulate S-cones and medium to long wave lengths stimulate M/L-cones. This spectral sensitivity is conferred by the protein part of the visual pigments, the opsin. Thus, opsins are slightly different, depending on their sensitivity and color preference. Each cone type carries a specific opsin. In rodents, S-cones express the ultraviolet-sensitive or SWS1 opsin,^{1,2} and M/L-cones express the LWS opsin,³ which detects only green light² and is known as L-opsin. Therefore, the strict nomenclature of these photoreceptors is L-cones. In some species, there are cones that coexpress both opsins; these are known as dual cones.⁴⁻⁶

The rat retina has been the subject of intensive research for several decades, because it is an easily accessible model for the study of the response of central nervous system neurons to a variety of insults and associated therapies.⁷⁻¹² It is, as well, a model for the study of experimentally induced photoreceptor degeneration, such as phototoxic insult,¹³ or that caused by inherited retinal diseases, such as retinitis pigmentosa¹⁴ or retinal dystrophy.^{15,16} Although there is a body of literature reporting the number and distribution of cones in several species of mammals,^{17,18} including pigs,¹⁹ primates,^{5,20-23} and several rodents,^{1,24-31} there is little information with respect to the common rat.^{3,32-35} Using immunohistochemical techniques, Szél and Rohlich³⁴ in 1992 reported the presence of S- and L-cones in the albino rat retina and estimated their proportions. Among cones, 6.7% were S-cones, giving a ratio of S- to L-cones of 1:15. According to their article, the greatest percentage of cones was found in the inferior and nasal retina, followed by the superior and temporal areas, although in the central retina few cones were detected. Last year, it was reported that the mean density of L-cones in the albino rat (Sprague-Dawley; SD) is approximately 2000 cells/mm²; however, no total number or spatial distribution was provided.³² Of importance, it has been demonstrated that, in the pigmented Long-Evans rat strain, these two types of cones allow dichromatic color vision.³

We have developed an automated method to quantify the total population of retinal ganglion cells (RGCs) that were identified by either retrograde tracing or immunohistofluorescence techniques.^{36,37} This approach allows the objective quantification of all the RGCs present in naïve or injured retinas and thus enables the assessment of RGC loss or the

From the ¹Fundación para la Formación e Investigación Sanitarias de la Región de Murcia, Murcia, Spain; ²Departamento de Oftalmología, Facultad de Medicina, Universidad de Murcia, Murcia, Spain; the Departments of ⁴Physiology and ⁵Ophthalmology, University of Alberta, Edmonton, Canada; and ⁶Hospital Universitario Virgen de la Arrixaca, Servicio Murciano de Salud, Murcia, Spain.

³Contributed equally to the work and therefore should be considered equivalent authors.

Supported by Research Grants 05703/PI/07 and 04446/GERM/07 from Fundación Séneca; FFIS-09/SMS01/BECA-08 Fundación para la Formación e Investigación Sanitarias de la Región de Murcia; SAF-2005-04812 Spanish Ministry of Education and Science; Spanish Ministry of Health and ISCIII-FEDER; PIO06/0780 and RD07/0062/0001, Red Temática de Investigación Cooperativa en Oftalmología.

Submitted for publication November 4, 2009; revised December 17, 2009; accepted December 17, 2009.

Disclosure: **A. Ortín-Martínez**, None; **M. Jiménez-López**, None; **F.M. Nadal-Nicolás**, None; **M. Salinas-Navarro**, None; **L. Alarcón-Martínez**, None; **Y. Sauvé**, None; **M.P. Villegas-Pérez**, None; **M. Vidal-Sanz**, None; **M. Agudo-Barriuso**, None

Corresponding author: Marta Agudo-Barriuso, Unidad de Investigación, Hospital Universitario Virgen de la Arrixaca, Servicio Murciano de Salud, Fundación para la Formación e Investigación Sanitarias de la Región de Murcia, 30.120 Murcia, Spain; martabar@um.es.

degenerative course after different insults.^{36,38,39} Moreover, the quantitative data aid in the construction of detailed isodensity maps illustrating the distribution of RGCs, as well as their density peaks. Based on our previous experience and taking advantage of the availability of commercial antibodies raised against the UV-sensitive opsin (S-cones) or the opsin red/green (L-cones), we proposed to double detect and quantify by an automated method, the whole population of S- and L-cones and to study their topographical distribution in flat-mounted retinas from two rat strains commonly used in the laboratory: one albino (Sprague-Dawley; SD) and the other pigmented (Piebald Virol Glaxo; PVG). The data gathered establish, for the first time, the normal values of both types of cones in adult rats and lay the foundations for further studies to analyze the effect of degenerative diseases, experimental insults, or ageing on each cone population.

MATERIAL AND METHODS

Animal Handling

All animals were treated in accordance with our institutional rules, European Union regulations, and the ARVO Statement for the Use of Animals in Ophthalmic and Vision Research. Adult rats of the SD and PVG strains were obtained from Harlan Laboratories, Inc. (Milan, Italy, [SD] and Longborough, UK [PVG]). The SD and PVG rats weighed 50 to 230 g (age, 3–3.5 months) and 80 to 160 g (age, 3–3.5 months), respectively.

Experimental Design

To study the S- and L-cone population, we used six retinas from each strain for radial sections and 12 (PVG) or 14 (SD) for analysis on whole, flat-mounted retinas. To quantify the total number of cones, we analyzed six whole, flat-mounted retinas from each strain. To study the correlation of RGCs and L-cone spatial distribution, we analyzed six additional retinas from each strain.

Double Immunohistofluorescence

All animals were deeply anesthetized with an overdose of sodium pentobarbital and perfused transcardially with 4% paraformaldehyde (PFA) in 0.1 M phosphate buffer after a saline rinse. After death, the superior pole of the eyes was sutured for posterior orientation, as described elsewhere.³⁸ The eyes were then enucleated and postfixed for 2 hours in 4% PFA at 4°C.

Oriented Radial Sections

The superior pole was labeled with yellow ink (Bradley Products, Inc., Bloomington, MI). The optic cups were dissected and cryoprotected in 15% sucrose (Sigma-Aldrich, Alcobendas, Madrid, Spain) before they were embedded, with the superior pole in known position, in optimal cutting temperature (OCT) compound (Sakura Finetek, Torrance, CA) for cryostat sectioning. Sections (15 μ m thick) were blocked in 5% normal donkey serum (NDS; Jackson ImmunoResearch Inc., Cambridge, UK) in phosphate buffered saline (PBS) with 0.1% Triton X-100. S- and L-opsins were double detected by an overnight incubation at 4°C with a mixture of the primary antibodies goat anti-OPN1SW (N-20), which detects the UV-sensitive opsin (i.e., S-cones; Santa Cruz Biotechnology, Heidelberg, Germany), and rabbit anti-opsin red/green, which detects the L-opsin in rodents (i.e., L-cones; Chemicon-Millipore Iberica, Madrid, Spain) diluted in blocking buffer (1:1100 for anti-OPN1SW and 1:1200 for anti-opsin red/green). Secondary detection was performed by incubating the sections, during 1 hour at room temperature, with Alexa Fluor-568 donkey anti-rabbit IgG (H+L) and Alexa Fluor-488 donkey anti-goat IgG (H+L; Molecular Probes-Invitrogen, Barcelona, Spain) each diluted 1:500 in PBS 0.1% Triton X-100. Finally, sections were thoroughly washed and mounted with anti-fade mounting medium containing DAPI, to counterstain the nuclei

(Vectashield mounting medium with DAPI; Vector Laboratories, Alicante, Spain).

Flat-Mounted Retinas

Retinas from both eyes were dissected as flattened whole-mounts, as previously reported.^{36–38} They were permeabilized in PBS 2% Triton by freezing them for 15 minutes at -70°C . After they were thawed at room temperature, the retinas were rinsed in new PBS-0.5% Triton. Primary and secondary detection was performed as for radial sections, with the exception that 2% Triton was used. In those retinas used to quantify the total number of cones, both opsins were detected with the same fluorophore, and thus, in these experiments, the secondary antibodies were Alexa Fluor-568 donkey anti-rabbit and Alexa Fluor-568 donkey anti-goat (Molecular Probes-Invitrogen), each diluted 1:500 in PBS 2% Triton. Finally, all retinas were thoroughly washed in PBS and mounted vitreal side down on subbed slides and covered with anti-fade mounting medium (Vectashield; Vector Laboratories).

Double immunodetection of L-cones and RGCs was performed as described, with the exception that the incubation with the primary antibodies was a mixture of goat anti-Brn3a (1:1000, Santa Cruz Biotechnologies) and of rabbit-anti opsin red/green (1:1200). In these immunodetections, Brn3a was detected in green (Alexa Fluor-488 donkey anti-goat) and opsin red/green in red (Alexa Fluor-568 donkey anti-rabbit). The retinas were mounted in anti-fade medium, vitreal side down, and the L-cone signal was acquired. Afterward, the retinas were mounted again, vitreal side up, to acquire the Brn3a signal.

Retinal Analysis

Whole-mounted retinas (left and right eyes) were analyzed for OPN1SW or Brn3a (detected with Alexa Fluor-488, i.e., green signal) and L-opsin (detected with Alexa Fluor-568, i.e., red signal). In the experiment performed to quantify the total number of cones, both opsins were detected in red. For the radial sections, S- and L-cone and DAPI signals were acquired. All images were taken with an epifluorescence microscope (Axioscop 2 Plus; Zeiss Mikroskopie, Jena, Germany) equipped with a computer-driven, motorized stage (ProScan H128 Series; Prior Scientific Instruments, Cambridge, UK), controlled by image-analysis software (Image Pro Plus software; IPP 5.1 for Windows; Media Cybernetics, Silver Spring, MD), as previously described.^{13,36,37} Briefly, to make reconstructions of retinal whole-mounts, we photographed retinal multiframe acquisitions for each fluorophore, in a raster scan pattern in which the frames were captured, with a $\times 10$ objective, contiguously, side-by-side, with no gap or overlap between them (Plan-Neofluar, 10×0.30 ; Zeiss Mikroskopie). Single frames were focused manually before the capture of the digitized images, which were then fed into the image-analysis program. Depending on the retina's size and orientation on the slide, a scan area is defined to cover the entire retina. This scan area consisted of a matrix of m-frames in columns and n-frames in rows, where the total number of frames in the scan area was indicated by frames in columns times frames in rows ($m \times n$). The frame size was 840×623 pixels, and 140 images usually were taken for each retina. The capture calibration was 1 pixel, which equals 0.0011 mm. The images taken for each retina were saved in a folder as a set of 24-bit color images. Later, these images were combined automatically into a single, tiled, high-resolution composite image of the whole retina (IPP 5.1 for Windows; Media Cybernetics). In this study, photomontages of radial sections were performed the same way as those of whole-mounted retinas, with the exception that the objective was $\times 20$, and, usually, 114 images were taken per section. Individual images, in flat-mounted or radial sections, were taken with an $\times 20$ or $\times 40$ objective, acquiring the red signal first; then, without moving the microscope stage, the green signal; and finally the blue (DAPI) signal, when needed. All images were captured at a resolution of 300 dpi. Reconstructed images were further processed with image-editing computer software (Adobe Photoshop CS; ver. 8.0.1; Adobe Systems, Inc., San Jose, CA), when correct orientation of the retina or image coupling was needed.

Image Processing: Automated Quantification of the Total Population of S-cones and L-cones in Whole-Mounted Retinas

To quantify the total number of S- and L-cones present in flat whole-mounted retinas, we developed an automated counting routine, using the macro language of the software (IPP for Windows; Media Cybernetics) for each type of cone. These routines counted positive cells in each of the 180 frames spanning a flat-mounted retina.

S-cones. In the first step, images were converted to 16-bit gray scale to discard color information, followed by the application of the flatten filter to eliminate luminosity variations in the image. The resulting image was then filtered with a top-hat filter, which enhances the brightness of objects over that of background. The S-cones were counted within predetermined parameters to exclude objects that were too large or too small to be outer segments. Finally, data of each count were displayed and exported by dynamic data exchange to a spreadsheet (Microsoft Office Excel 2003; Microsoft Corp.), and the data were filed and saved for further analysis.

L-cones. In a first step, the images were converted to 16-bit gray scale to discard color information. The flatten filter was applied on the gray-scale image to eliminate luminosity variations in the image. Then, a best fit was performed to enhance the positive objects, followed by use of an enhancement filter (HiGauss, IPP software; Media Cybernetics), which highlights the image by using a Gaussian filtering method. Finally, data of each count were displayed and exported by dynamic data exchange to a spreadsheet (Microsoft Office Excel 2003; Microsoft Corp.), and the data were filed and saved for further analysis. This routine was used, as well, to quantify the total number of cones (S+L+dual) detected with the same fluorophore.

Brn3a. Automated quantification of Brn3a-positive RGCs was performed according to a published method.³⁶

Validation of the S- and L-cones Automated Counting Methods

To validate both automated counting methods, three different experienced investigators counted manually, in a masked fashion, a total of 50,695 L-cones and 8,077 S-cones present in 22 frames. These frames represented different density regions and were randomly selected from eight whole-mounted retinas. The automated quantification of these images resulted in 51,928 and 8,130 L- and S-cones, respectively. Finally, each automated method was statistically compared (SigmaStat for Windows ver. 3.11; Systat Software, Inc., Richmond, CA) to its manual counterpart, and a correlation coefficient of 0.99 (Pearson correlation test $R^2 = 0.986$) was obtained for the L-cones automated routine and of 0.98 (Pearson correlation test $R^2 = 0.977$) for the S-cones automated routine. Thus, both automated counting methods were reliable and valid.

Manual Quantification and Topographical Distribution of Dual Cones

The presence of dual cones, that is to say cones that express both opsins, was observed in both rat strains. These cones were manually quantified, in the same six representative retinas per strain for which isodensity maps were generated, as follows: At first the retinal whole-mount images for the S (green signal) and L (red signal) cones were edited and coupled (Adobe Photoshop). Then, the whole retina was examined at high magnification, frame by frame. Every dual cone, detected because the co-localization of both opsins was yellow, was dotted in a new layer. Afterward, a counting routine was developed (Image Pro Plus macro language; Media Cybernetics) and launched, to quantify the number of dots (dual cones), as described elsewhere.⁴⁰ The layer with the dots was extracted and resized, to illustrate their topographical distribution.

Retinal Area Measurement

The area of each whole-mounted retina was measured on the high-resolution photomontage image of the complete retina, with the software (IPP; Media Cybernetics) calibrated off the stage movement.

Isodensity Maps

Detailed topographical distribution of S- and L-cones was demonstrated with isodensity maps in six retinas from each strain: three right and three left. These maps were constructed as previously described for RGCs,^{36,37} with the exception that each original frame was divided into 25 sampling areas instead of 64. These maps are filled contour plots generated by assigning to each one of the 25 subdivisions of each frame a color code according to its cone density, within a 28-step, color-scale range from 0 (purple) to 6500 or higher (red) L-cones/mm² in both rat strains. There is a significantly higher number of S-cones in the albino than in the pigmented strain; therefore, to appreciate the spatial distribution in both strains, a different density scale was given to each one. Thus, in the albino strain, the scale was from 0 (purple) to 1300 or higher (red) S-cones/mm², whereas in the pigmented strain, red was set at values of 900 or higher S-cones/mm². Isodensity maps of Brn3a-positive RGCs were generated, as previously described.³⁶

Statistical Analysis

The analysis of the differences between groups of retinas or groups of animals was performed with the Mann-Whitney or *t*-tests (SigmaStat for Windows, ver. 3.11; Systat Software, Inc.). Data are shown as the mean \pm SEM, and differences are considered significant at $P < 0.05$.

RESULTS

Identification of S- and L-cones in Oriented Retinal Radial Sections

The first objective was to analyze the expression pattern of both opsins in oriented radial sections. Figure 1 shows the double detection of the UV-sensitive opsin (green signal) and L-opsin (red signal) in the retina of the albino rat, and Figure 2 shows these findings in the retina of the pigmented strain. The images in both Figures 1 and 2 show the expression patterns of both opsins in different areas of the retina: dorsal (B, C, F, G, J, K), ventral (D, E, H, I, L, M), peripheral (B, E, F, I, J, M), and central (C, D, G, H, K, L). There was a mutually exclusive labeling of cone subpopulations, demonstrating that each antibody recognized a different opsin. In both strains, opsin expression was confined to the external segments of the S (UV-sensitive opsin) and L (L-opsin) cones, although at lower antibody dilutions, the cone somata and the synaptic terminals were also detected (not shown). At this low dilution, the L-opsin antibody faintly recognized, in both strains, cells located in the ganglion layer, which have been described and are known as atypical cones.⁴¹

We observed as well that both types of cones were distributed throughout the retinal section and that the L-cones were more abundant than the S-cones. A closer inspection of the coupled images disclosed that some cones expressed both opsins, which means that, in adult SD and PVG rats (yellow signal, arrows in Figs. 1J, 2J), there were dual cones (addressed in detail later). In this analysis, no differences were found in the two strains in the expression pattern of opsins and distribution of S- and L-cones.

Identification of S- and L-cones in Flat-Mounted Retinas

Next, we proposed to detect both types of cones in flat-mounted retinas. The results of this experiment are illustrated in Figure 3. These images correspond to eight areas of the

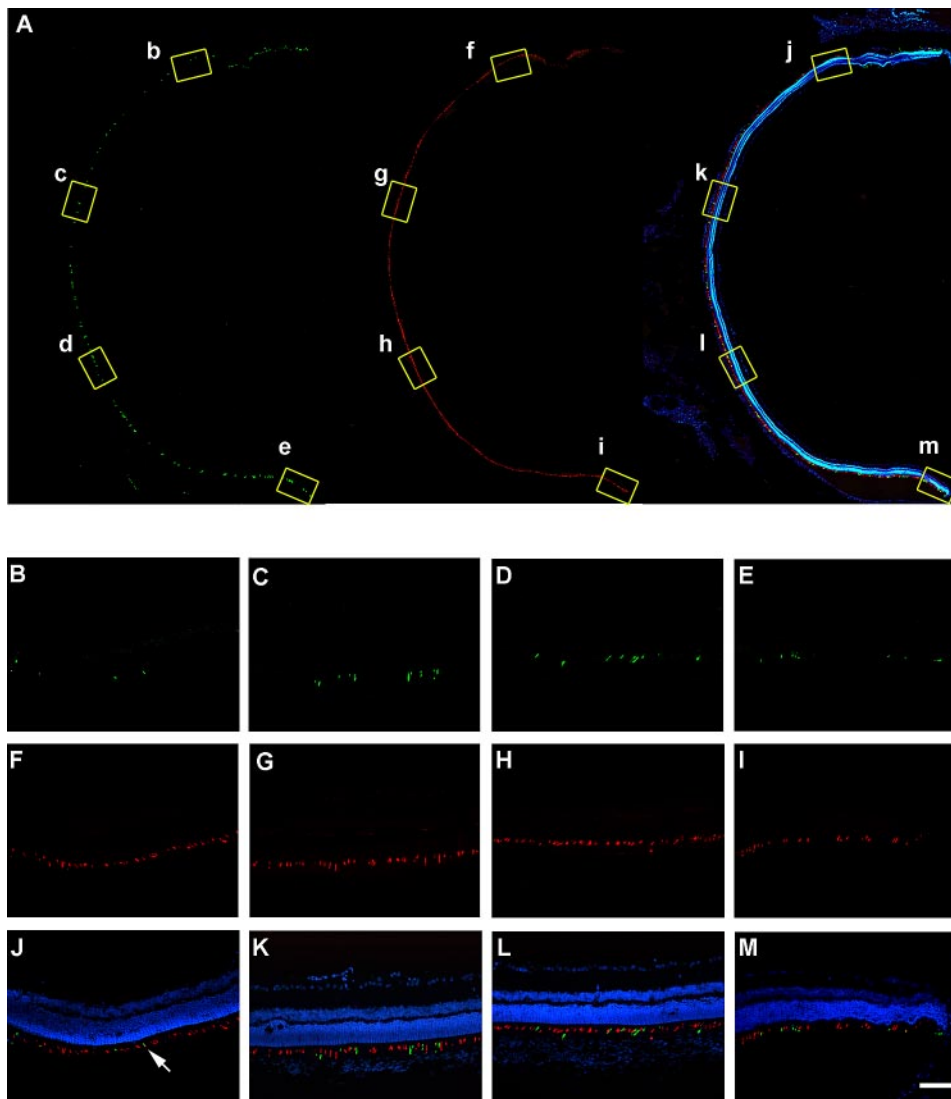


FIGURE 1. Immunodetection of S- and L-cones in oriented retinal radial sections from SD rats. **(A)** Photomontage of an oriented radial section from an SD rat retina spanning the optic nerve. The superior pole is located at 12 o'clock. These sections were immunoreacted for UV-sensitive opsin, which is expressed in S-cones (*left, green* signal) and L-opsin which is expressed in L-cones (*middle, red* signal). These images were coupled with the nuclear stain DAPI (*blue*) in the *right* image. **(B–I)** Magnifications corresponding, respectively, to the squares **(b–i)** shown in **(A)**. **(B–E)** Immunodetection of S-cones, **(F–I)** immunodetection of L-cones; **(J, K)** coupled images showing S- and L-cones and DAPI counterstaining. *Arrows*: dual cones. Bar, 100 μ m.

retina (Fig. 3A–H from SD and 3I–P from PVG rats) as follows: two images, one central and one peripheral, were acquired for each one of the four retinal quadrants (superior, inferior, nasal, and temporal). Central images were taken at 1 mm from the optic nerve and peripheral ones at the retinal border. In both rat strains, we observed that the S-cones were more abundant in the peripheral than in the central retina in all retinal quadrants (compare green signal in Figs. 3A, 3B, 3E, 3F, 3I, 3J, 3M, 3N with the green signal in 3C, 3D, 3G, 3H, 3K, 3L, 3O, 3P). In fact, S-cone density seemed higher in the far retinal periphery and the retinal rim (see gradient from top to bottom in Figs. 3A, 3B, 3E, 3F, 3I, 3J, 3M, 3N). Besides, when comparing the quantity of S-cones detected in each strain, it seemed that these were more abundant in the SD than in the PVG rats (compare Figs. 3C, 3D, 3G, 3H with 3K, 3L, 3O, 3P). The L-cones were more abundant in the central than in the peripheral retina (compare red signal in Figs. 3C, 3D, 3G, 3H, 3K, 3L, 3O, 3P to red signal in Figs. 3A, 3B, 3E, 3F, 3I, 3J, 3M, 3N), and no clear differences are observed between the strains.

In agreement with the radial section results, L-cones were more abundant than S-cones (compare green to red signal) and, although most of the cones in both strains were genuine S- or L-cones—that is, cones that expressed only one opsin (higher magnification in Fig. 3Q)—some cones were dual (i.e., expressed both opsins; Figs. 3R–T, arrows).

Automated Quantification of the Whole Population of S- and L-cones

To quantify the total number of S- and L-cones, we developed two automated counting routines using the macro language of commercial software (IPP for Windows; for details and validation of each routine, see the Material and Methods section). Figure 4 shows a representative left whole-mounted retina of each rat strain (SD, Figs. 4A, 4B; PVG, Figs. 4C, 4D) where the S (Figs. 4A, 4C) and the L (Figs. 4B, 4D) cones were doubly detected. The number of S- and L-cones counted in each retina is also shown. It is worth highlighting that, because double immunodetection was performed, both types of cones were counted in the same retinas. In total, S- and L-cones from 14 SD and 12 PVG retinas were quantified (Table 1A, Fig. 4). The mean number \pm SEM of S-cones counted in the SD and PVG strains was $41,028 \pm 5,074$ and $27,316 \pm 2,235$, respectively. The difference in the total number of S-cones in both strains is statistically significant (Mann-Whitney test; $P < 0.001$). The mean \pm SEM number of L-cones was $231,736 \pm 14,517$ and $239,939 \pm 6,494$ in the SD and PVG rats, respectively; the difference was not significant (Mann-Whitney test; $P = 0.227$). Therefore, the ratio of S- to L-cones was $1:5.7 \pm 0.6$ and $1:8.7 \pm 2.9$ in the SD and PVG strains, respectively.

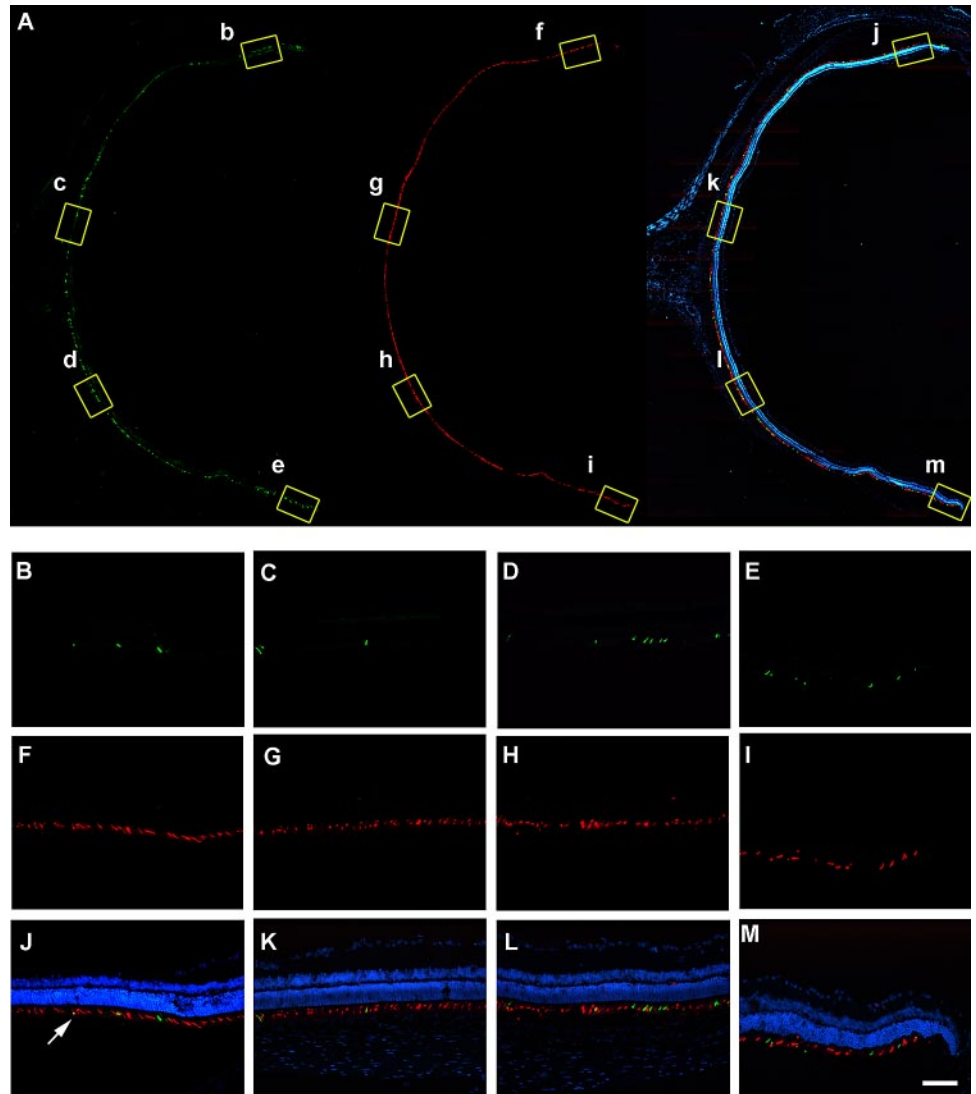


FIGURE 2. Immunodetection of S- and L-cones in oriented retinal radial sections from PVG rats. The remainder of the description is as in Figure 1.

Because it was also possible to determine the area of each retina, the mean density of both cones was calculated, and so in the SD strain, there was a mean \pm SEM of 689 ± 84 S-cones/mm² and of 3906 ± 358 L-cones/mm², whereas in the pigmented strain their density was 442 ± 43 S-cones/mm² and 3878 ± 167 L-cones/mm². In conclusion, in both rat strains there were more L- than S-cones; furthermore, the albino strain had a significantly higher number of S-cones than did the pigmented one.

Topographical Distribution of the Whole Population of S-cones

The next step was to analyze the spatial distribution of each cone type in both rat strains. For this analysis, we generated isodensity maps based on the quantification data (for explanations see the Material and Methods section). Figure 5 shows the topography of S-cones in six retinas, three left and three right, from each strain (SD, Figs. 5A-F; PVG, Figs. 5G-L). According to these maps, S-cones were similarly distributed in both rat strains. Their highest densities (red, 1300 or higher S-cones/mm² in the SD strain, and 900 or higher S-cones/mm² for the pigmented rat) were found on the far retinal periphery and retinal rims (100–50 μ m from the retinal end), both superior and inferior, although this distribution was more evident in the superior retina. Their lowest densities (blue) were found in

the superior retina in the area from the optic nerve to the retinal edge. In the inferior retina, the S-cones were of intermediate density (green, yellow). Finally, an increase in the density of these cones was noted toward the inferonasal quadrant (orange).

Topographical Distribution of the Whole Population of L-cones

Figure 6 shows the topography of L-cones in the three left and three right retinas from the same SD (Figs. 6A-F) and PVG (Figs. 6G-L) rats as are shown in Figure 5. As observed for the S-cones, there were no differences between the strains in the pattern of L-cone distribution. L-cones were distributed in a fashion that seemed to be complementary of the topography of S-cones; that is, their lowest densities were found in the retinal borders (blue); the medium densities (green, yellow) were located in the medial, superior, and inferior retina; and the highest densities (orange, red) are observed above the optic nerve, along the nasotemporal axis. This distribution was easily observed when looking at the patterns of both types of cones in the same retina (for example, Figs. 5A and 6A, and so on for each panel in each figure). Of interest, the highest densities (red) were found within the central region, above the optic nerve along the nasotemporal axis, mimicking the spatial distribution of retinal ganglion cells described by our group,

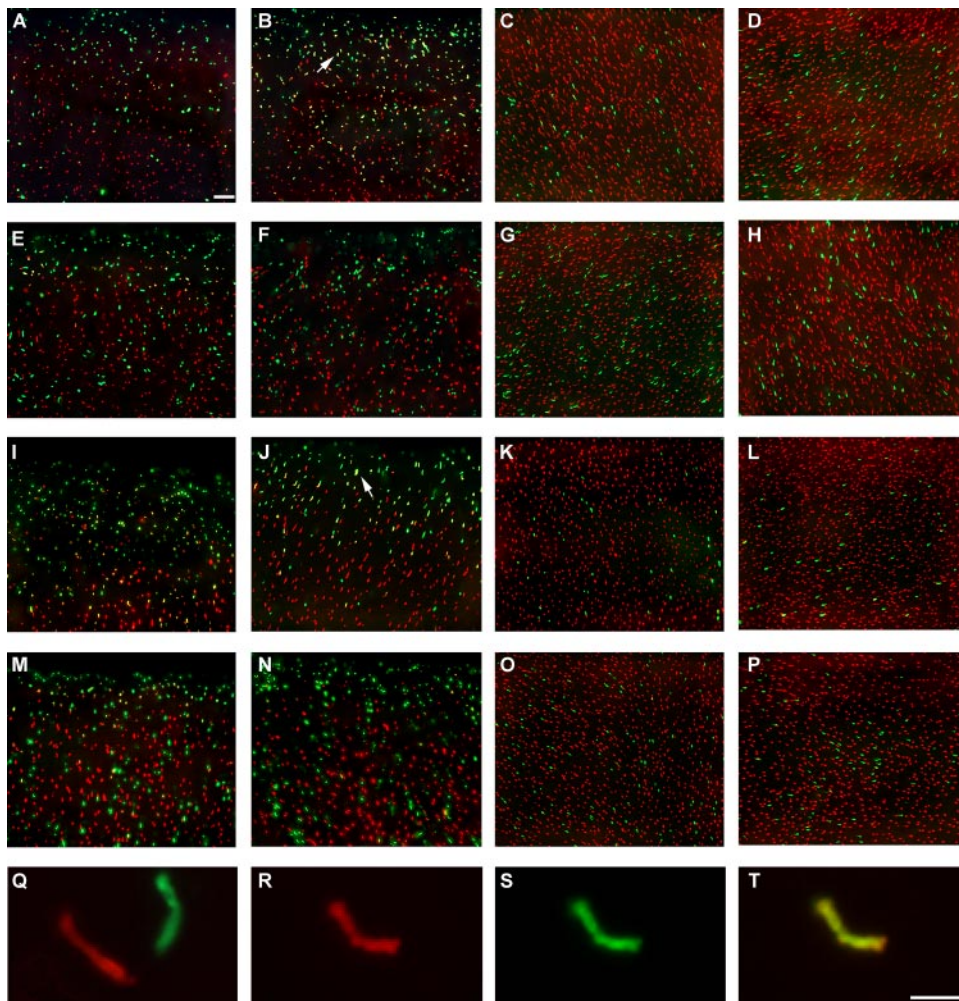


FIGURE 3. Immunodetection of S- and L-cones in flat-mounted retinas from SD and PVG rats. Immunodetection of S (green signal) and L (red signal) cones in flat-mounted retinas from SD (A–H, Q–R) and PVG (I–P) rats. Images in (A, B, E, F, I, J, M, N) correspond to the periphery (retinal rim) of each one of the four retinal quadrants (superotemporal: A, I; inferotemporal: E, M; superonasal: B, J; and inferonasal: F, N). All images are oriented from the retinal border (top) to the medial retina (bottom). Images in (C, D, G, H, K, L, O, P) correspond to the central retina (1 mm from the optic nerve) of the same quadrants (superotemporal: C, K; inferotemporal: G, O; superonasal: D, L; and inferonasal: H, P). Most of the cones in both rat strains, express one opsin, either S (green signal) or L (red signal), these were genuine S- or L-cones, respectively (magnification in Q). However, dual cones were also identified (arrows and magnifications in R–T), these cones express L-opsin (R) and S-opsin (S). In (T) is shown the coupled image (R+S). Bar: (A–P) 100 μ m; (Q–T) 50 μ m.

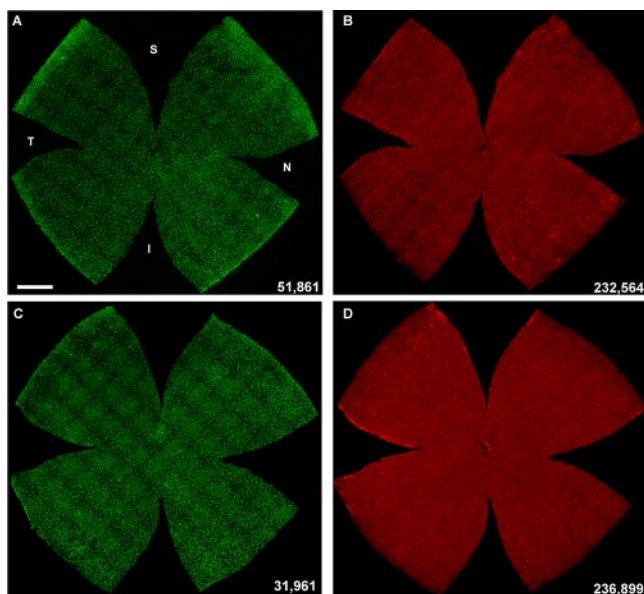


FIGURE 4. Quantification of the total population of S- and L-cones in SD and PVG whole-mounted retinas. Whole-mounts of representative left SD (A, B) and PVG (C, D) retinas where the S-cones (A, C) and the L-cones (B, D) were double immunodetected. Bottom right of each map: the number of S- or L-cones counted in that retina. S, superior; I, inferior; T, temporal; N, nasal. Bar, 1 mm.

which are also densest in this retinal area.^{36,37} This phenomenon is addressed in detail in the next section.

Quantification and Topographical Distribution of the Whole Population of Dual Cones

Because dual cones were detected, it was of interest to know how many of them there were and where in the retina they were located. In the same 12 retinas ($n = 6$ per strain) from which the S and L isodensity maps were obtained, dual cones were manually dotted on the retinal photomontage, and these dots were quantified by our automated system. The mean \pm SEM number of dual cones was 8607 ± 3325 and 7758 ± 1182 in the SD and PVG rats, respectively (Table 1A). Of note, the mean percentage of dual cones, with respect to the total number of cones, was close to a 3% in both rat strains (Figs. 7A, 7B). This approach may underestimate the number of dual cones in this species, since only yellow cones in the coupled images (red+green signal) were indicated by the dots, which means that only those cones with a similar expression of both opsins were counted. Thus, it is possible that there were dual cones that coexpressed both opsins, with the expression of one of them being below the detection sensitivity of the protocol. For the assessment of this possibility, confocal analysis would probably render better results; however, this method is not feasible since, to capture the whole retina, at least 180 individual images are needed. Nevertheless, quantification of the total number of cones (see below) showed that these numbers are quite accurate.

TABLE 1. Total Number of Dual, S-, L-, Genuine S-, and Genuine L-cones and Total Cone Counts in the SD and PVG Rats

A. The Total Number of S- and L-cones Quantified in the Same Retina by an Automated Routine

	Cones (n)							Densities (mm ²)					
	S-cones	L-cones	Dual Cones	Genuine S-cones (S-dual)	Genuine L-cones (L-dual)	Estimated Total	Retinal Area (mm ²)	S-cones	L-cones	Dual	Genuine S-cones	Genuine L-cones	Estimated Total/mm ²
SD rats													
Right retinas													
1	30,930	219,094	—	—	—	—	59	521	3,694	—	—	—	—
2	43,228	259,988	—	—	—	—	59	729	4,382	—	—	—	—
3	50,209	233,429	12,617	37,592	220,812	271,021	63	802	3,728	201	600	3,526	4,302
4	40,769	243,301	—	—	—	—	63	650	3,879	—	—	—	—
5	31,910	251,770	—	—	—	—	55	582	4,594	—	—	—	—
6	48,517	245,152	14,574	33,943	230,578	279,095	62	788	3,980	237	551	3,743	4,502
7	37,135	213,334	4,876	32,259	208,458	245,593	61	613	3,519	80	532	3,439	4,026
Left retinas													
8	51,861	232,564	5,660	46,201	226,904	278,765	60	864	3,874	94	770	3,779	4,646
9	34,928	200,876	—	—	—	—	60	584	3,361	—	—	—	—
10	36,474	220,445	7,608	28,866	212,837	249,311	60	611	3,696	128	484	3,568	4,155
11	44,435	225,897	6,309	38,126	219,588	264,023	61	727	3,696	103	624	3,593	4,328
12	41,285	248,575	—	—	—	—	57	721	4,339	—	—	—	—
13	39,530	209,149	—	—	—	—	65	606	3,208	—	—	—	—
14	43,180	240,723	—	—	—	—	51	850	4,740	—	—	—	—
Mean	41,028	231,736	8,607	36,165	219,863	264,635	60	689	3,906	141	593	3,608	4,327
SEM	5,074	14,517	3,325	4,475	6,235	11,659	2	94	358	52	71	102	165
PVG rats													
Right retinas													
1	26,977	247,199	4,820	22,157	242,379	269,356	60	447	4,098	80	367	4,018	4,489
2	23,895	251,489	—	—	—	—	64	371	3,902	—	—	—	—
3	30,877	250,270	—	—	—	—	60	517	4,190	—	—	—	—
4	25,265	233,830	—	—	—	—	58	433	4,003	—	—	—	—
5	32,002	233,310	8,735	23,267	224,575	256,577	59	546	3,980	149	397	3,831	4,349
6	27,657	244,286	7,155	20,502	237,131	264,788	67	416	3,670	108	308	3,563	3,952
Left retinas													
7	25,655	245,112	9,482	16,173	235,630	261,285	60	429	4,100	159	271	3,942	4,355
8	25,761	226,294	7,213	18,548	219,081	244,842	63	409	3,590	114	294	3,475	3,886
9	25,389	235,397	—	—	—	—	62	409	3,794	—	—	—	—
10	24,862	234,941	—	—	—	—	63	397	3,756	—	—	—	—
11	31,961	236,899	8,061	23,900	228,838	260,799	62	517	3,830	130	386	3,699	4,206
12	27,494	240,243	—	—	—	—	66	415	3,626	—	—	—	—
Mean	27,316	239,939	7,578	20,758	231,272	259,608	62	442	3,878	123	337	3,755	4,206
SEM	2,235	6,494	1,182	2,350	7,108	5,932	2	43	167	23	46	176	191

For this experiment S-cones were detected in green and L-cones in red. The number of dual ones was assessed with a semiautomated method. The number of genuine S- and genuine L-cones was calculated by subtracting the number of S- and L-cones from the number of dual cones. The estimated number of total cones is the sum of dual, genuine S- and genuine L-cones. Each retinal area was automatically measured, which allowed calculating the densities of each cone type. At the bottom of each column is shown the mean ± SEM.

B. Total Number of Cones (S+L+dual)

Rat Strain	Total Number of Cones Per Retina						Mean	SEM
	1	2	3	4	5	6		
SD	259,564	268,118	262,277	254,759	270,157	265,374	263,375	4,508
PVG	243,268	255,632	237,642	284,153	261,109	264,615	257,737	12,223

For this quantification, S, L and dual cones were detected using the same fluorophore; hence, all cones were labeled in red, whether they express one or both opsins. These cones were automatically quantified. Mean and SEM values are shown at the right of the table.

As observed in Figures 8A-L, dual cones were similarly distributed in both rat strains. These images indicate that the dual cones were more abundant in the retinal far periphery, close to the retinal rim, the areas where the S-cones were denser. It is worth highlighting that, even though most of

the dual cones were found in the far retinal periphery, they did not reach the retinal rim, where most of the cones were genuine S-cones (Fig. 8M). In the rest of the retina, however, they were homogeneously distributed, with no resemblance to the S (superior void and inferonasal gradient) or L (naso-

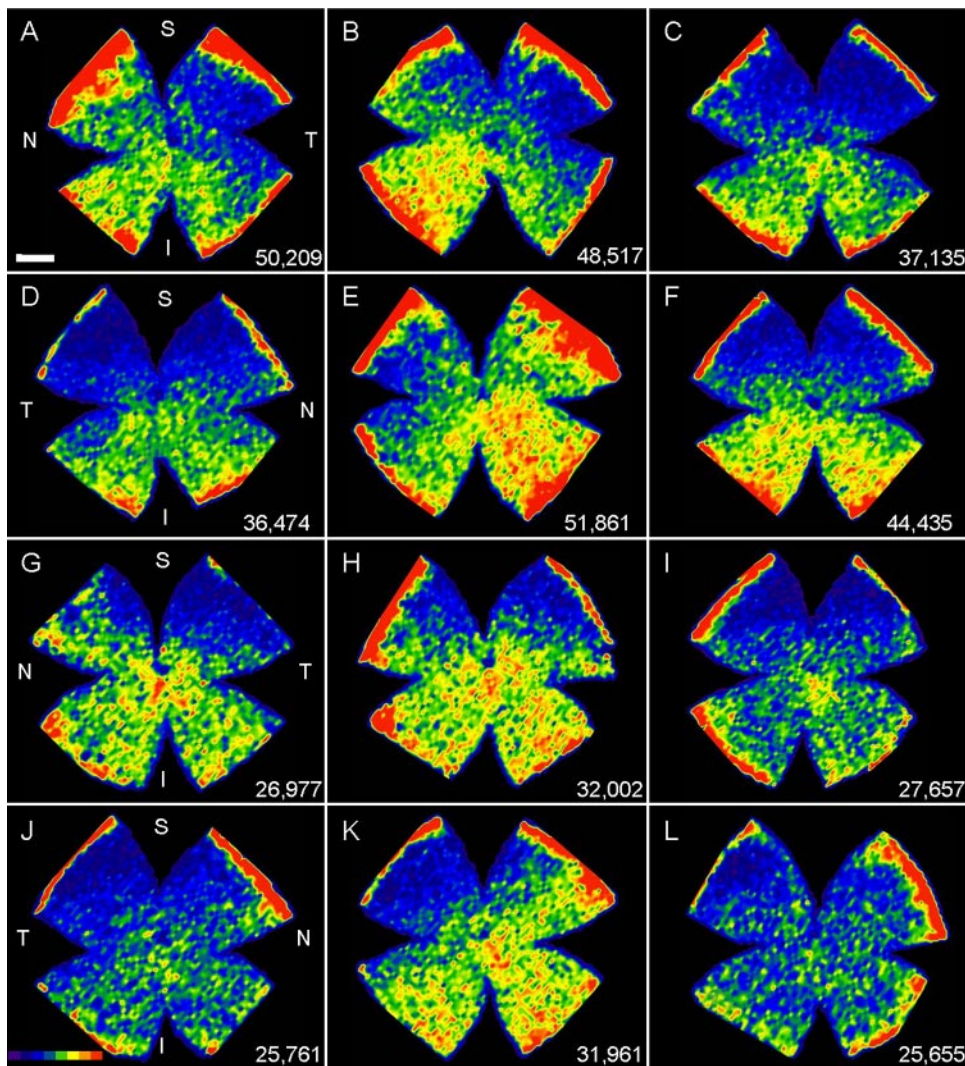


FIGURE 5. Topographical distribution of S-cones in SD and PVG rats. Isodensity maps showing the distribution of S-cones in the SD (A–F) and PVG (G–L) strains. (A–C, G–I) Right retinas; (D–F, J–L) left retinas. The maps are filled contour plots generated by assigning to each of the 25 subdivisions of each frame a color code according to its cone density value within a color-scale range from 0 (purple) to 1300 or more (red) S-cones/mm² in the SD rat and from 0 (purple) to 900 or more (red) S-cones/mm² in the PVG strain. In the PVG rat, there were fewer S-cones than in the SD one, and for that reason, the color scale range is lower. *Bottom right* of each map: the number of S-cones counted in that section. S, superior; T, temporal; I, inferior; N, nasal.

temporal axis) cone topography shown in Figures 5 and 6, respectively.

Numbers and Ratios of Genuine S- and L-cones and of Total Cones

Because, as mentioned, the number of dual cones may have been underestimated, in six retinas from each strain, both opsins were detected with the same fluorophore. In this manner, all cones were detected in red, irrespective of their opsin expression. Results from the automated quantification of cones thus detected (genuine S+genuine L+dual) are shown in Table 1B. These data show that the total number of cones did not differ from the estimated population of cones calculated by adding up the number of genuine S, genuine L, and dual cones (Table 1A). These results indicate that most, if not all, of the dual cones were identified in the double-immunodetection experiment (Table 1B).

If the total number of cones is taken into account, there were no significant differences (*t*-test; $P = 0.461$) between the strains, as the SD strain had a mean number of cones of $263,3756 \pm 4,508$ and the PVG strain of $257,737 \pm 12,223$. Thus, the percentage of L- and S-cones with respect to the total number of cones was, respectively, 87.5% and 15.5% in the albino strain and 92.4% and 10.5% in the pigmented one (Fig. 7).

Knowing the number of dual cones present in both rat strains enabled calculating the number of genuine S- and L-

cones (Table 1) by mere subtraction of the number of dual cones from the total number of S- or L-cones. Thus, these counts were $36,165 \pm 4,475$ and $219,863 \pm 17,765$ in the albino rat and $20,758 \pm 2,350$ and $231,272 \pm 7,108$ in the pigmented strain, respectively. Statistically, the number of genuine S-cones in the albino strain is significantly higher than in the pigmented rat (Mann-Whitney test; $P < 0.001$), and the number of genuine L-cones present in the PVG rat is significantly higher ($P = 0.042$) than in the SD strain. When only the number of genuine cones is considered, the ratio of S- to L-cones is 1:5.2 and 1:8.5 in the albino and pigmented strain, respectively and their percentage with respect to the total number of cones is, respectively, 83% and 14% in the albino strain and 89% and 9% in the pigmented rat—ratios and percentages close to those calculated when all the S- and L-cones are taken into account (Fig. 7).

Parallel Distribution of RGCs and L-cones

The spatial distribution of L-cones in both rat strains mimics the spatial distribution of RGCs described in detail by our group.^{36,37,42} To further analyze this possible co-distribution, double immunolabeling of RGCs (Figs. 9E, 9F) and L-cones was carried out in the same retinas, both types of cells quantified, and isodensity maps generated (Figs. 9A–D). The isodensity maps showed, first, that RGCs (Fig. 9A, SD strain; and 9C, PVG strain) were distributed throughout the whole retinal surface

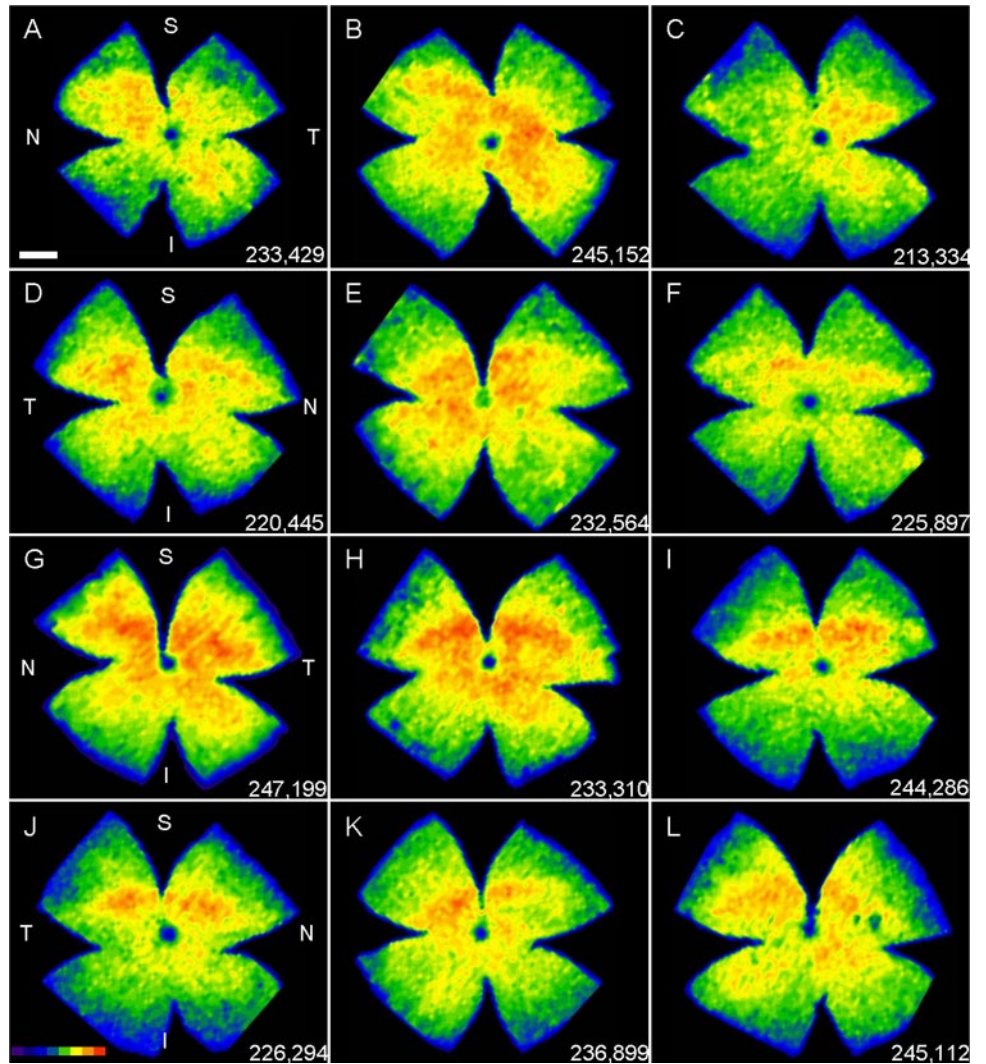


FIGURE 6. Topographical distribution of L-cones in SD and PVG rats. Isodensity maps of the same retinas from Figure 5 showing the distribution of L-cones in the SD (A–F) and PVG (G–L) strains. (A–C, G–I) Right retinas; (D–F, J–L) left retinas. The maps are filled contour plots generated by assigning to each of the 25 subdivisions of each frame a color code according to its cone density value within a color-scale range from 0 (purple) to 6500 or more L-cones/mm². Bottom right of each map: the number of L-cones counted in that retina. S, superior; T, temporal; I, inferior; N, nasal.

and, in agreement with our previous work, that their topography was not homogeneous, as they were densest along the superior nasotemporal axis, an area that has been proposed to be the visual streak in rodents,^{36,37,42} and, second, that L-cone distribution (SD, Fig. 9B; PVG, 9D) matched that of RGCs, as their density peak was found in the same area (Fig. 9, compare isodensities A with B and C with D). Furthermore, we observed that RGC and L-cone co-distribution expanded across the entire retinal surface, as high and low densities of each cell type

followed the same pattern in both topographies, indicating that, in those areas where there were more L-cones, there are also more RGCs.

Quantitatively, the total number of RGCs in the SD retina was 82,158 and in the PVG retina was 85,117 (Figs. 9A, 9C, respectively), in accordance with our previous work, were a mean of 83,449 Brn3a⁺ RGCs in the SD rats³⁶ and 85,341 in the PVG rats (Nadal-Nicolás et al., unpublished data, 2009, *n* = 7 retinas) was reported. In these retinas, the number of L-cones

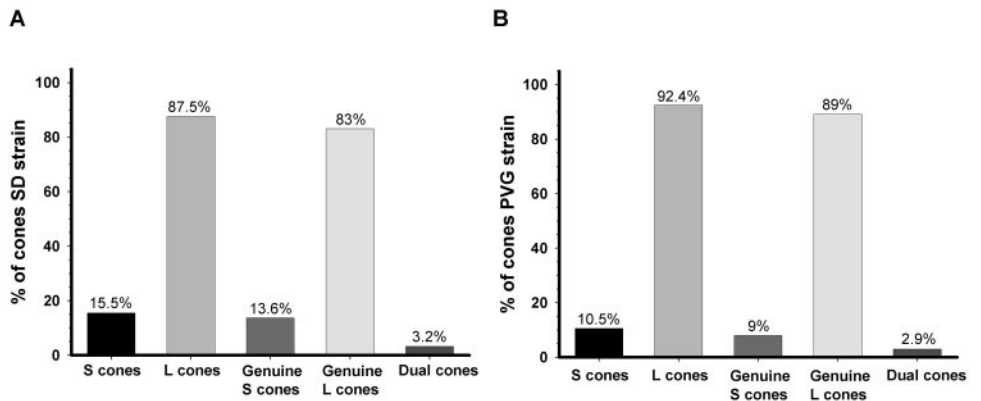


FIGURE 7. Percentage of S, L, genuine S, genuine L, and dual cones in the SD (A) and PVG (B) rat strains, with respect to the total cone population (considered 100%).

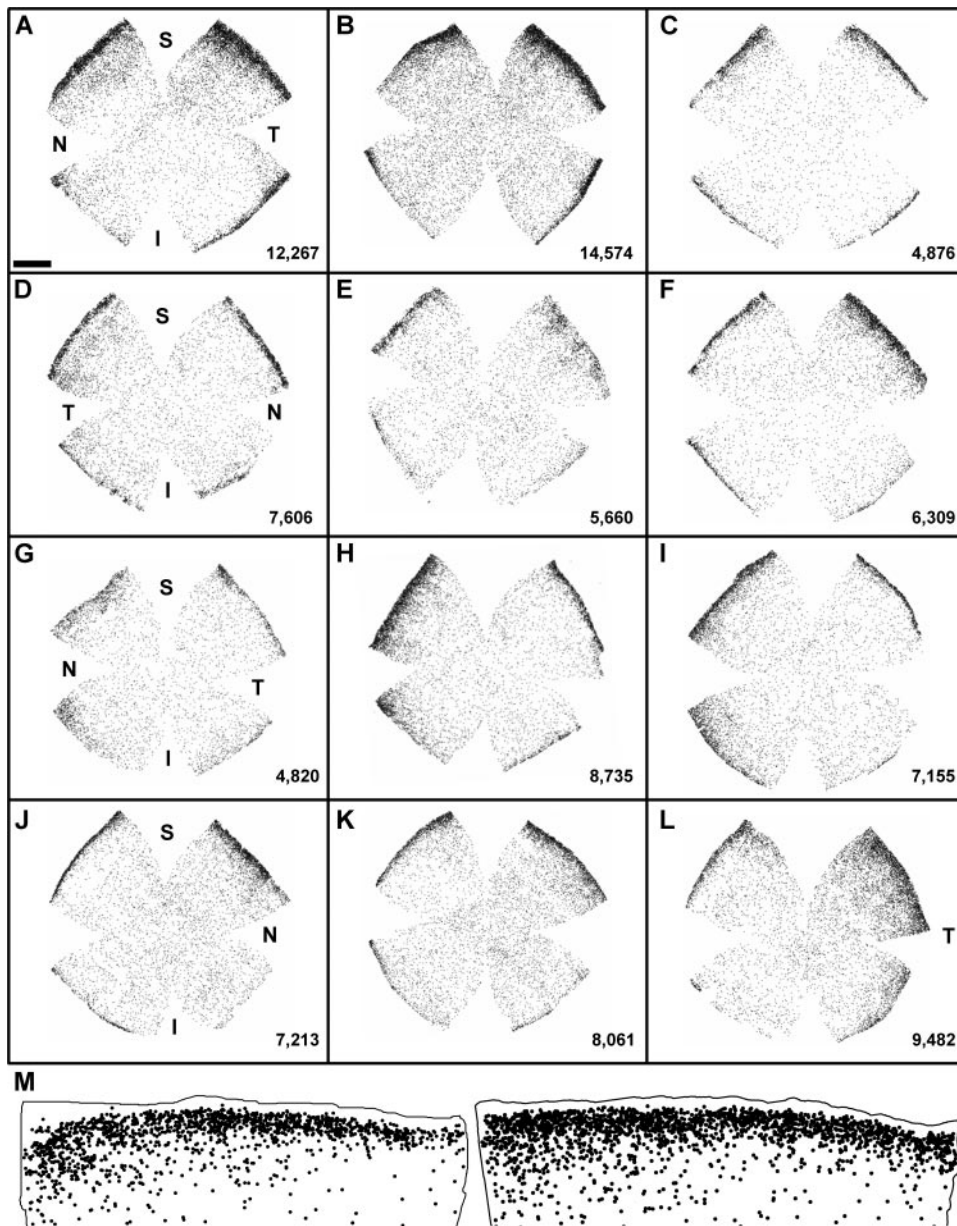


FIGURE 8. Topographical distribution of dual cones in SD and PVG rats. Plots depicting the spatial distribution of dual cones in the six SD (A–F) and six PVG (G–L) retinas shown in Figures 5 and 6, respectively. (A–C, G–I) Right retinas; (D–F, J–L) left retinas. These images were extracted from the original retinas where the dual cones were dotted. *Bottom right* of each map: the number of dual cones counted in each retinal section. (M) Magnifications of the retinal border, showing that, while dual cones reach the far periphery, the retinal rim is devoid of them. S, superior; T, temporal; I, inferior; N, nasal.

was 215,739 in the SD strain and 239,502 in the PVG one (Figs. 9C and 9D, respectively). Considering the mean number of RGCs^{36,37} and of L-cones shown in this work, there was a ratio of RGCs to L-cones of 1:2.8 in both strains, or ~ 1 RGC for 3 L-cones.

DISCUSSION

The retina of the common rat, *Rattus norvegicus*, is widely used in studies aimed at increasing the understanding of induced^{13,43} or inherited^{14,16,44} retinal degenerations that affect photoreceptors. However, there is little information regarding the number and distribution of cone photoreceptors in this species.^{1,3,34,35} Our work determined, for the first time, the total cone counts and total number and the detailed topographical distribution of S- and L-cones present in adult animals from two inbred laboratory rat strains: one albino and one pigmented. In addition, we demonstrated the presence of dual cones in adult rats, their number, and their retinal distribution. Finally, we provided direct evidence that the topography of

L-cones parallels the spatial distribution of RGCs. These data and approaches may be used as baseline and hallmark to reliably quantify, in rats, the degeneration of each type of cone associated with different insults¹³ or mutations¹⁵ as well as to assess the effects of neuroprotective therapies on the survival of each cone type.

To our knowledge, there is one report³ in which an approximate density of cones in the Long-Evans pigmented strain is given (from 2000 to 7000 [S+L]/mm²). They also report that S-cones were, in this pigmented strain, approximately 10% of the cone population (ratio S:L-cones 1:10). These data are in agreement with the results presented herein, albeit in a different pigmented strain. With respect to the albino rat, there is a recent article³² reporting a density of L-cones in SD rats of ~ 2000 cells/mm². This density is lower than that reported herein, but they sample the retina while we quantify the whole L-cone population. Our quantification data in the albino strain cannot be compared with the classical work by Szel and Röhlich,³⁴ as they show the proportion of S- and L-cones and rods related to the 5000 photoreceptors counted, rather than

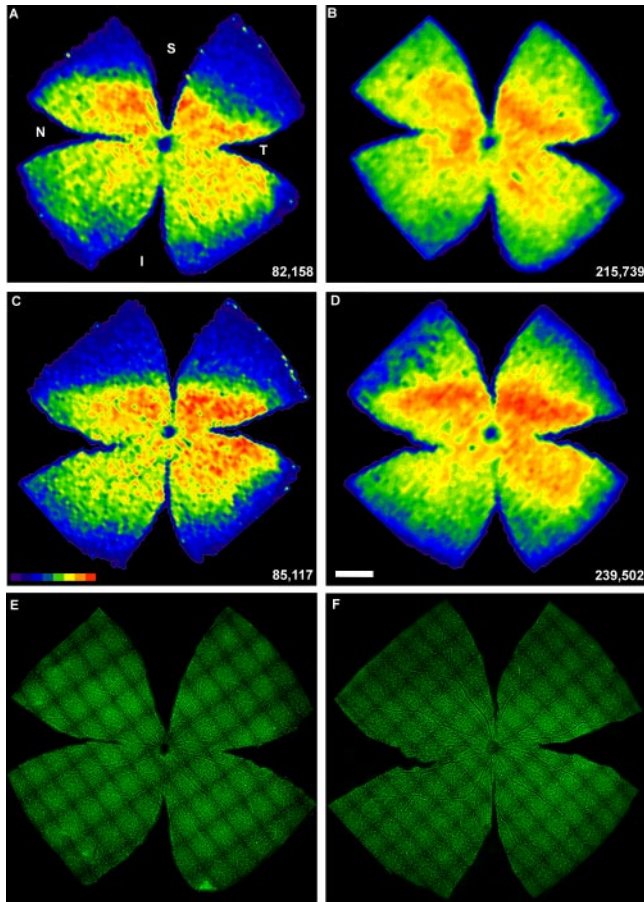


FIGURE 9. Parallel distribution of retinal ganglion cells and L-cones in SD and PVG rats. (A, B) Isodensity maps of the same SD retina showing the topographical distribution of RGCs (A) and L-cones (B). (C, D) Isodensity maps of the same PVG retina showing the topographical distribution of RGCs (C) and L-cones (D). (E, F) Retinal photomontages showing Brn3a immunodetection. These retinas correspond to the isodensity maps in (A) and (C), respectively. *Bottom right* of each map: number of RGCs or L-cones counted in that retina. These isodensities are filled contour plots generated by assigning to each one of the subdivisions of each frame a color code according to its RGC or L-cone density value within a color-scale range from 0 (purple) RGCs or L-cones/mm² to 3000 or higher RGCs/mm² (red; A, C) or 7000 or higher L-cones/mm² (red; B, D). S, superior; T, temporal; I, inferior; N, nasal. Scale bar, 1 mm.

density or total numbers. In this study, the percentage of S-cones accounted for 6% to 7% of the total cone population, which gives a ratio of S:L-cones of 1:15, a ratio higher than ours. Regarding cone distribution, Szel et al.³⁴ have observed that these cells are not evenly distributed in the retina, being more abundant in the inferior nasal region, a distribution that does not fully agree with our isodensity maps. Finally, this group³⁵ detected in young albino rats, but not in adult animals, the presence of dual cones, again in apparent conflict with our data. These discrepancies are now discussed.

According to the general rule observed in most mammalian species,⁵ both rat strains have an L-cone-dominant retina, where the number of L-cones exceeds that of S-cones by a ratio of 6:1 and 9:1 in the albino or pigmented strain, respectively, a ratio that in the albino rat is lower than the ratio of 10:1 found in most species, including the rat.^{3,5,34} The ratios shown herein are calculated from the mean number of each type of cone. However, because S- and L-cones are not homogeneously distributed in the retina, and in fact, the distribution of S-cones

in these two rat strains is the reverse of the distribution of L-cones, as has been described in rabbits, the tarsier, mouse, and lemur,^{18,20,45} the S-to-L-cone ratio changes in different regions of the retina. For instance, in the retinal rim, the S-cones peak, with densities of 1300 or 900 S-cones/mm² or more in the albino and pigmented rat, respectively (Fig. 6, red). In this same area, the L-cones have their lowest values, from 800 to 1600 cones/mm² (Fig. 8, blue), in both strains. Thus, assuming the lowest values, in the retinal rim the ratio of L- to S-cones would decrease to 0.7:1 and 1:1 in the albino and pigmented strains, respectively. If we consider the cone densities in the dorsomedial retina, where the L-cones peak and there is an absence of S-cones, this picture changes and the L- to S-cone ratio goes up to 15:1 and 27:1 in the albino and pigmented rat, respectively. The numerical differences with Szel and Rohlich,³⁴ may be explained by the approach used in each work, as we quantified the total population of both types of cones and assessed their topographical distribution based on these data, rather than sampling the retina.

The different S-to-L ratio between both strains is explained by the only quantitative difference observed in them: The albino strain has a significantly higher number of S-cones than does the pigmented one and, in turn, the latter has a higher number of L-cones. The biological meaning of these differences is unknown, but they may be related to the differences in photopic visual function observed between albino and pigmented rats.^{33,34}

There were no differences in the total number of cones between both strains or in the spatial distribution of each type of cone. In fact, in both strains, the S pigment dominates the peripheral retina, whereas the L pigment is preferentially expressed in the medial and central retina. This rough distribution is widespread in most of the mammalian species with separate cone populations, including primates and humans.¹⁸

S-cones are densest in the far retinal periphery and retinal rims, both superior and inferior. Although cone-rich rims have been described in humans^{23,46} and recently in rats,¹⁶ this is the first time that the existence of an S-cone rim in the four retinal quadrants has been fully documented, probably because the whole retina was analyzed. The function of the cone-rich rim remains a matter for discussion,⁴⁶ and indeed it is not known whether these cones are functional at all. However, Vugler et al.¹⁶ have reported that melanopsin-expressing RGCs form a well-organized plexus at the retinal border that mirrors the S-cone rich rim, an arrangement that has also been observed in the cone-rich fovea of primates.⁴⁷ This finding leads to the hypothesis that the S-cone-rich rim in rats may be related to the function of melanopsin-expressing RGCs, which play a role in driving the circadian and the pupillomotor systems.⁴⁷ The medium S-cones densities are found in the inferior retina, more so in the nasal quadrant. The lowest S-cone density is found in the dorsal-central retina, where the L-cones and RGCs are densest. This finding is very interesting, because this area has been proposed to be the visual streak of rats.³⁷ The visual streak is a region of the retina specialized to provide the best vision at some point in the visual space. In primates, some birds, and reptiles, this rounded area is known as the area centralis. The main characteristic of the visual streak is that it contains a high concentration of RGCs, L-cones, and bipolar cells, but is mostly devoid, in adult primates including humans, of S-cones and rods.^{5,48} Although the densities of bipolar cells and rods are not accounted for herein, we showed that in this dorsal area above the optic nerve, both L-cones and RGCs reach their maximum densities, whereas the S-cones reach their lowest, thus further supporting the role of this retinal region as the visual streak in rats. Moreover, our data demonstrate, for the first time, that in both rat strains, L-cones parallel the distribution of RGCs, as has been observed in primates

(reviewed in Ref. 49). Furthermore, the quantification of the total population of both types of neurons gives a ratio of 1 RGC to 3 L-cones. This ratio was fairly conserved throughout the retinal surface, since, as shown in Figure 9, the density peaks and valleys of both cell types are found in the same retinal regions.

The presence of dual cones has been reported for several species of mammals, (reviewed in Ref. 5 including mice^{4,6,50}). In mice, most of the cones are dual, but this opsin co-expression does not impair dichromatic color discrimination.⁵⁰ In contrast with Szel et al.³⁵ we found dual cones to be present in the adult rat retina. These cones account for 3% of the total cones in both rat strains and are found highly packaged in the retinal far periphery, superior and inferior retina, but homogeneously distributed in the medial and central retina. This pattern does not fit with any of the five patterns of dual cone distribution reviewed by Lukats et al.⁵ It has, however, characteristics of human retinas, where dual cones are uniformly distributed throughout the entire whole retina.

In conclusion, in this work, we established for the first time the total cone counts and the total number of S- and L-cones as well as of dual cones, together with their detailed topography, in two rat strains: pigmented and albino. Furthermore, we demonstrated that RGCs and L-cone spatial distributions match, with both cell types densest in the visual streak of the rat. Altogether, these data provide the normal values of both types of cones in adult rats and are the pillar that will support further studies analyzing the effects of degenerative diseases, experimental insults, or ageing on each cone population.

Acknowledgments

The authors thank Anthony Vugler for his advice on the anti-UV-sensitive opsin antibody and Leticia Nieto-López and Isabel Cánovas-Martínez for expert technical support.

References

- Szel A, Rohlich P, van Veen T. Short-wave sensitive cones in the rodent retinas. *Exp Eye Res.* 1993;57:503-505.
- Bowmaker JK, Hunt DM. Evolution of vertebrate visual pigments. *Curr Biol.* 2006;16:R484-R489.
- Jacobs GH, Fenwick JA, Williams GA. Cone-based vision of rats for ultraviolet and visible lights. *J Exp Biol.* 2001;204:2439-2446.
- Applebury ML, Antoch MP, Baxter LC, et al. The murine cone photoreceptor: a single cone type expresses both S and M opsins with retinal spatial patterning. *Neuron.* 2000;27:513-523.
- Lukats A, Szabo A, Rohlich P, Vigh B, Szel A. Photopigment co-expression in mammals: comparative and developmental aspects. *Histol Histopathol.* 2005;20:551-574.
- Rohlich P, van Veen T, Szel A. Two different visual pigments in one retinal cone cell. *Neuron.* 1994;13:1159-1166.
- Aviles-Trigueros M, Sauve Y, Lund RD, Vidal-Sanz M. Selective innervation of retinorecipient brainstem nuclei by retinal ganglion cell axons regenerating through peripheral nerve grafts in adult rats. *J Neurosci.* 2000;20:361-374.
- Whiteley SJ, Sauve Y, Aviles-Trigueros M, Vidal-Sanz M, Lund RD. Extent and duration of recovered pupillary light reflex following retinal ganglion cell axon regeneration through peripheral nerve grafts directed to the pretectum in adult rats. *Exp Neurol.* 1998;154:560-572.
- Vidal-Sanz M, De la Villa P, Aviles-Trigueros M, et al. Neuroprotection of retinal ganglion cell function and their central nervous system targets. *Eye.* 2007;21:S42-S45.
- Aguayo AJ, Vidal-Sanz M, Villegas-Perez MP, Bray GM. Growth and connectivity of axotomized retinal neurons in adult rats with optic nerves substituted by PNS grafts linking the eye and the midbrain. *Ann NY Acad Sci.* 1987;495:1-9.
- Sasaki H, Coffey P, Villegas-Perez MP, et al. Light induced EEG desynchronization and behavioral arousal in rats with restored retinocollicular projection by peripheral nerve graft. *Neurosci Lett.* 1996;218:45-48.
- Vidal-Sanz M, Lafuente MP, Mayor S, de Imperial JM, Villegas-Perez MP. Retinal ganglion cell death induced by retinal ischemia: neuroprotective effects of two alpha-2 agonists. *Surv Ophthalmol.* 2001;45(suppl 3):S261-S267.
- Marco-Gomariz MA, Hurtado-Montalban N, Vidal-Sanz M, Lund RD, Villegas-Perez MP. Phototoxic-induced photoreceptor degeneration causes retinal ganglion cell degeneration in pigmented rats. *J Comp Neurol.* 2006;498:163-179.
- Sancho-Pelluz J, Arango-Gonzalez B, Kustermann S, et al. Photoreceptor cell death mechanisms in inherited retinal degeneration. *Mol Neurobiol.* 2008;38:253-269.
- Villegas-Perez MP, Vidal-Sanz M, Lund RD. Mechanism of retinal ganglion cell loss in inherited retinal dystrophy. *Neuroreport.* 1996;7:1995-1999.
- Vugler A, Semo M, Joseph A, Jeffery G. Survival and remodeling of melanopsin cells during retinal dystrophy. *Vis Neurosci.* 2008;25:125-138.
- Ahnelt PK, Schubert C, Kubber-Heiss A, Schiviz A, Anger E. Independent variation of retinal S and M cone photoreceptor topographies: a survey of four families of mammals. *Vis Neurosci.* 2006;23:429-435.
- Peichl L. Diversity of mammalian photoreceptor properties: adaptations to habitat and lifestyle? *Anat Rec A Discov Mol Cell Evol Biol.* 2005;287:1001-1012.
- Hendrickson A, Hicks D. Distribution and density of medium- and short-wavelength selective cones in the domestic pig retina. *Exp Eye Res.* 2002;74:435-444.
- Hendrickson A, Djajadi HR, Nakamura L, Possin DE, Sajuthi D. Nocturnal tarser retina has both short and long/medium-wavelength cones in an unusual topography. *J Comp Neurol.* 2000;424:718-730.
- Jacobs GH. Primate color vision: a comparative perspective. *Vis Neurosci.* 2008;25:619-633.
- Szel A, Lukats A, Fekete T, Szepessy Z, Rohlich P. Photoreceptor distribution in the retinas of subprimate mammals. *J Opt Soc Am A Opt Image Sci Vis.* 2000;17:568-579.
- Williams RW. The human retina has a cone-enriched rim. *Vis Neurosci.* 1991;6:403-406.
- Bobu C, Lahmam M, Vuille P, Ouarour A, Hicks D. Photoreceptor organization and phenotypic characterization in retinas of two diurnal rodent species: potential use as experimental animal models for human vision research. *Vision Res.* 2008;48:424-432.
- Gaillard F, Bonfield S, Gilmour GS, et al. Retinal anatomy and visual performance in a diurnal cone-rich laboratory rodent, the Nile grass rat (*Arvicanthis niloticus*). *J Comp Neurol.* 2008;510:525-538.
- Gaillard F, Kuny S, Sauve Y. Topographic arrangement of S-cone photoreceptors in the retina of the diurnal Nile grass rat (*Arvicanthis niloticus*). *Invest Ophthalmol Vis Sci.* 2009;50:5426-5434.
- Glosmann M, Steiner M, Peichl L, Ahnelt PK. Cone photoreceptors and potential UV vision in a subterranean insectivore, the European mole. *J Vis.* 2008;8:1-12.
- Lukats A, Dkhissi-Benyahya O, Szepessy Z, et al. Visual pigment coexpression in all cones of two rodents, the Siberian hamster, and the pouched mouse. *Invest Ophthalmol Vis Sci.* 2002;43:2468-2473.
- Neitz M, Neitz J. The uncommon retina of the common house mouse. *Trends Neurosci.* 2001;24:248-250.
- Peichl L, Nemeč P, Burda H. Unusual cone and rod properties in subterranean African mole-rats (Rodentia, Bathyergidae). *Eur J Neurosci.* 2004;19:1545-1558.
- Szel A, Csorba G, Caffè AR, Szel G, Rohlich P, van Veen T. Different patterns of retinal cone topography in two genera of rodents, *Mus* and *Apodemus*. *Cell Tissue Res.* 1994;276:143-150.
- Chrysostomou V, Stone J, Valter K. Life history of cones in the rhodopsin-mutant P23H-3 rat: evidence of long-term survival. *Invest Ophthalmol Vis Sci.* 2009;50:2407-2416.
- Heiduschka P, Schraermeyer U. Comparison of visual function in pigmented and albino rats by electroretinography and visual evoked potentials. *Graefes Arch Clin Exp Ophthalmol.* 2008;246:1559-1573.

34. Szel A, Rohlich P. Two cone types of rat retina detected by anti-visual pigment antibodies. *Exp Eye Res.* 1992;55:47-52.
35. Szel A, van Veen T, Rohlich P. Retinal cone differentiation. *Nature.* 1994;370:336.
36. Nadal-Nicolas FM, Jimenez-Lopez M, Sobrado-Calvo P, et al. Brn3a as a marker of retinal ganglion cells: qualitative and quantitative time course studies in naive and optic nerve-injured retinas. *Invest Ophthalmol Vis Sci.* 2009;50:3860-3868.
37. Salinas-Navarro M, Mayor-Torroglosa S, Jimenez-Lopez M, et al. A computerized analysis of the entire retinal ganglion cell population and its spatial distribution in adult rats. *Vision Res.* 2009;49:115-126.
38. Salinas-Navarro M, Alarcon-Martinez L, Valiente-Soriano FJ, et al. Ocular hypertension impairs optic nerve axonal transport leading to progressive retinal ganglion cell degeneration. *Exp Eye Res.* 2010;90(1):168-183.
39. Salinas-Navarro M, Alarcon-Martinez L, Valiente-Soriano FJ, et al. Functional and morphological effects of laser-induced ocular hypertension in retinas of adult albino Swiss mice. *Mol Vis.* 2009;15:2578-2598.
40. Parrilla-Reverter G, Agudo M, Nadal-Nicolas F, et al. Time-course of the retinal nerve fibre layer degeneration after complete intra-orbital optic nerve transection or crush: a comparative study. *Vision Res.* 2009;49(23):2808-2825.
41. Semo M, Vugler AA, Jeffery G. Paradoxical opsin expressing cells in the inner retina that are augmented following retinal degeneration. *Eur J Neurosci.* 2007;25:2296-2306.
42. Salinas-Navarro M, Jimenez-Lopez M, Valiente-Soriano FJ, et al. Retinal ganglion cell population in adult albino and pigmented mice: a computerized analysis of the entire population and its spatial distribution. *Vision Res.* 2009;49:637-647.
43. Wenzel A, Grimm C, Samardzija M, Reme CE. Molecular mechanisms of light-induced photoreceptor apoptosis and neuroprotection for retinal degeneration. *Prog Retin Eye Res.* 2005;24:275-306.
44. Pennesi ME, Nishikawa S, Matthes MT, Yasumura D, LaVail MM. The relationship of photoreceptor degeneration to retinal vascular development and loss in mutant rhodopsin transgenic and RCS rats. *Exp Eye Res.* 2008;87:561-570.
45. Juliusson B, Bergstrom A, Rohlich P, Ehinger B, van Veen T, Szel A. Complementary cone fields of the rabbit retina. *Invest Ophthalmol Vis Sci.* 1994;35:811-818.
46. Mollon JD, Regan BC, Bowmaker JK. What is the function of the cone-rich rim of the retina? *Eye* 1998;12:548-552.
47. Dacey DM, Liao HW, Peterson BB, et al. Melanopsin-expressing ganglion cells in primate retina signal colour and irradiance and project to the LGN. *Nature.* 2005;433:749-754.
48. Rodieck RW. *The First Steps in Seeing.* Sunderland, MA: Sinauer Associates, Inc.; 1998.
49. Schulte D, Bumsted-O'Brien KM. Molecular mechanisms of vertebrate retina development: implications for ganglion cell and photoreceptor patterning. *Brain Res.* 2008;1192:151-164.
50. Jacobs GH, Williams GA, Fenwick JA. Influence of cone pigment coexpression on spectral sensitivity and color vision in the mouse. *Vision Res.* 2004;44:1615-1622.